

# Simulation and experimental study of ultra-low temperature heat transfer characteristics of continuous heat exchangers in the dilution refrigerator

Haowen Guo<sup>1,2</sup>, Ruixin Li<sup>1</sup>, Lingjiao Wei<sup>1,\*</sup>, Houlei Chen<sup>1</sup>, Jingtao Liang<sup>1,2</sup>, Zijie Pan<sup>1</sup>, Maowen Zheng<sup>1</sup>, Miguang Zhao<sup>1</sup> and Jiarun Zou<sup>1</sup>

1State Key Laboratory of Cryogenic Science and Technology, Technical Institute of Physics and Chemistry, Chinese Academy of Sciences, Beijing, China

2University of Chinese Academy of Sciences, Beijing, China

\*E-mail: weilingjiao@mail.ipc.ac.cn

**Abstract.** Dilution refrigerators, which can continuously obtain a minimum temperature of 10 mK, are key refrigeration systems in quantum computing. The continuous heat exchanger is an indispensable core component in the dilution refrigerator, which pre-cools the incoming concentrated <sup>3</sup>He liquid by exchanging heat with the return mixture. This study develops a thermodynamic model that incorporates flow heat transfer and Kapitza thermal resistance, analyzing the effect of heat exchanger length on performance. Simulations under flow rates of 0.3-1.0 mmol/s indicate that outlet temperatures decrease with increasing length, with an optimal length around 9-10 meters. An experimental continuous heat exchanger of 10-meter length was fabricated using copper-nickel tubing and integrated into a dry dilution refrigerator. Experimental results show actual outlet temperatures between 56-78 mK, slightly lower than simulated values due to thermal coupling with subsequent silver powder heat exchangers and the mixing chamber. The system achieved a cooling capacity of 450  $\mu$ W at 100 mK, demonstrating the model's practical utility. The research in this paper effectively improves the performance of dilution refrigerators and provides guidance for the design of our future dilution refrigerators.

## 1. Introduction

The rapid development of quantum computing has recently created a high demand for ultra-low temperature environments. Integrating large-scale quantum chips requires refrigeration systems with high stability and sufficient cooling capacity. Dilution refrigerators are the core equipment for achieving the sub-Kelvin temperature region and can stably provide the necessary low-temperature environment for superconducting quantum computation [1].

In the dilution refrigeration process, the circulating <sup>3</sup>He gas is pre-cooled and passes through the flow resistance and then through the still chamber and the counter-current heat exchanger in turn before entering the mixing chamber. In the mixing chamber, <sup>3</sup>He atoms enter the dilute phase from the concentrated phase via the phase separation interface, which is generated by gravity. This process produces a refrigeration effect, reaching a temperature of approximately 10 mK [2].



Content from this work may be used under the terms of the [Creative Commons Attribution 4.0 licence](https://creativecommons.org/licenses/by/4.0/). Any further distribution of this work must maintain attribution to the author(s) and the title of the work, journal citation and DOI.

Therefore, to improve the performance of the dilution cooler, a counter-current heat exchanger with good heat transfer properties is required [3]. The continuous heat exchanger is the first part of the counter-current heat exchanger and plays an important role in precooling  $^3\text{He}$ . Optimizing its heat transfer performance affects the performance of the entire dilution refrigerator.

This paper considers the coupled effects of axial heat transfer and Kapitza thermal resistance of liquid helium in a continuous heat exchanger to construct a flow heat transfer equation for numerical solutions. Heat transfer at different flow rates and lengths is analyzed to determine the optimal length. Thus, a continuous heat exchanger is designed, and its performance is verified and analyzed through experimentation. This will serve as a guide for designing future dilution refrigerators.

## 2. Continuous heat exchanger model

### 2.1. Structural model

In the dilution refrigerator, the counter-current heat exchanger is principally connected to the still chamber and the mixing chamber. The concentrated  $^3\text{He}$  phase exits the heat exchange tube in the still chamber, while the dilute phase flows from the diluted  $^3\text{He}$ - $^4\text{He}$  mixture in the mixing chamber, with counter-current heat transfer occurring between these phases. The primary objective of this process is to pre-cool the incoming flow of  $^3\text{He}$  liquid. The continuous heat exchanger is connected to the outlet of the still, which initially cools down the incoming  $^3\text{He}$ . In this study, a continuous heat exchanger model is constructed, and the following assumptions are made to facilitate the analysis in combination with the actual situation:

1. It is assumed that the flow on the concentrated phase side as well as on the dilute phase side is laminar, disregarding all forms of disturbances in the flow process. The flow is regarded as stable.
2. It is assumed that the temperature remains constant within a specific cross-section. In this process, the effects of fluid viscosity and radial thermal conduction are disregarded.
3. The thermal resistance of the copper-nickel material between the concentrated phase side and the dilute phase side of the flow process is negligible; therefore, the average Kapitza thermal resistance is employed for calculation.
4. The flow of the concentrated phase and dilute phase in the spiral tube is estimated as horizontal direct flow, with the effect produced by the spiral being disregarded.
5. The inlet temperature of the concentrated phase pipe is 700 mK, and the outlet temperature of the dilute phase pipe is 20 mK.

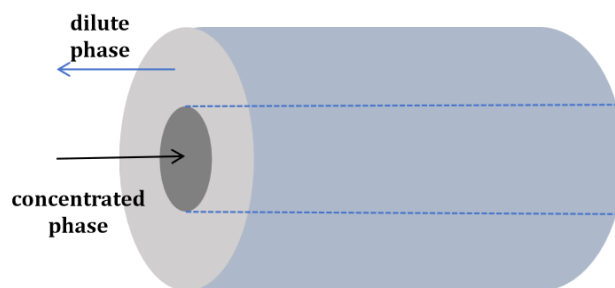


**Figure 1.** Schematic of the continuous heat exchanger.

As illustrated in Figure 1, the continuous heat exchanger is depicted schematically. According to the equation of conservation of energy, and combined with the aforementioned assumptions, the temperature relationship between the concentrated phase side and the dilute phase side can be obtained as equation (1) and (2) as follows [4]:

Concentrated phase side:

$$\rho_c C_c u_c \frac{\partial T_c}{\partial x} = \frac{\partial}{\partial x} \left( k_c \frac{\partial T_c}{\partial x} \right) + S_c \quad (1)$$

Dilute phase side:

$$\rho_d C_d u_d \frac{\partial T_d}{\partial x} = \frac{\partial}{\partial x} \left( k_d \frac{\partial T_d}{\partial x} \right) + S_d \quad (2)$$

The above two formulas describe the heat transfer in concentrated and dilute phases. In these formulas,  $\rho$  represents the density of the fluid,  $C$  represents the specific heat capacity of the fluid,  $u$  represents the flow rate of the fluid, and  $k$  represents the thermal conductivity of the fluid. According to the aforementioned equation,  $S$  represents the source term, which is generated by the process of heat exchange between the concentrated phase and the dilute phase within the continuous heat exchanger. In consideration of the Kapitza thermal resistance at ultra-low temperatures, the source term can be expressed as follows [5]:

$$S_c = \frac{(T_d^4 - T_c^4)}{2R_{km}r} \quad (3)$$

$$S_d = \frac{(T_c^4 - T_d^4)}{2R_{km}r} \quad (4)$$

In the equation (3) and (4),  $R_{km}$  represents the average Kapitza thermal resistance on both sides of the concentrated and dilute phases, while  $r$  represents the average radius. At ultra-low temperatures, the specific heat capacity and the thermal conductivity undergo changes, rendering them unsuitable as constants for calculation. The following Table 1 [4-6] lists the parameters required for the calculation.

Table 1. Physical parameters of concentrated and dilute phases at low temperatures

Parameters	Concentrated phase	Dilute phase
Density $\rho$ (kg·m <sup>-3</sup> )	92.4	143.9
Specific heat capacity $C$ (J·kg <sup>-1</sup> ·K <sup>-1</sup> )	$7.87 \times 10^3 \times T$	$27.16 \times 10^3 \times T$
Thermal conductivity $k$ (W·m <sup>-1</sup> ·K <sup>-1</sup> )	$33 \times 10^3 \times T^{-1}$	$23 \times 10^4 \times T^{-1}$

In the theoretical analysis, the concentrated phase tube has an inner diameter of 1 mm and an outer diameter of 1.5 mm, while the dilute phase tube has an inner diameter of 5.4 mm and an outer diameter of 6 mm. Based on the sub-finite difference discretization of the aforementioned equations, the windward format is used for the convenience of the solution.

## 2.2. Simulation result

The flow rates of 0.3, 0.5, 0.7, and 1.0 mmol/s with different heat exchanger lengths are calculated, and the results obtained are shown in Figure 2. As illustrated in Figure 2, the outlet temperature of the continuous heat exchanger exhibits a decline with an increase in the heat exchange length. This phenomenon displays a distinct trend: a rapid decrease in the initial stage and a subsequent gradual decrease in the subsequent stage. It has been demonstrated that an increase in the circulating flow rate corresponds to an increase in the outlet temperature. It can be determined that the optimal length for the heat exchanger is between 9 and 10 meters. An insufficient length will result in inadequate heat transfer, while an excessively long length will impact the available space, with no discernible enhancement in performance. Increases in the circulating flow rate necessitate the implementation of a longer heat transfer length.

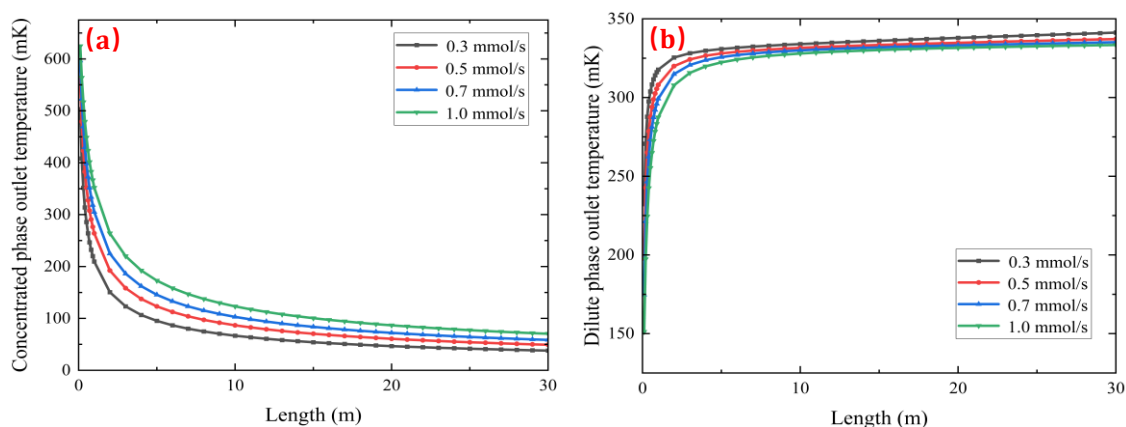


**Figure 2.** In Continuous heat exchangers, the outlet temperatures of the concentrated phase and dilute phase at different flow rates and lengths, with concentrated phase inlet temperature of 700 mK and dilute phase inlet temperature of 20 mK.

### 3. System experiment

Preliminary findings from the simulation in the previous section indicate that the system utilizes a continuous heat exchanger composed of copper-nickel material. The dilute phase tube possesses an inner diameter of 5.4 mm, an outer diameter of 6 mm, and a length of 3 meters. In comparison, the dilute phase tube has an inner diameter of 1 mm, an outer diameter of 1.5 mm, and a length of 10 meters, which is coiled in the form of a helix to augment the process of heat exchange. This can be regarded as having a 10-meter heat transfer length, consistent with the structure of the preceding section of the analysis. The continuous heat exchanger utilized is illustrated in Figure 3.



**Figure 3.** Continuous heat exchanger

#### 3.1. Experimental systems

The experimental tests were conducted in a dry dilution refrigerator. The refrigerator is composed primarily of a two-stage GM pulse tube refrigerator, a J-T heat exchanger, a still, a continuous heat exchanger, a silver powder heat exchanger, a mixing chamber, flanges at all levels, and support rods. Figure 4 illustrates the dilution unit assembled with the continuous heat exchanger previously described.

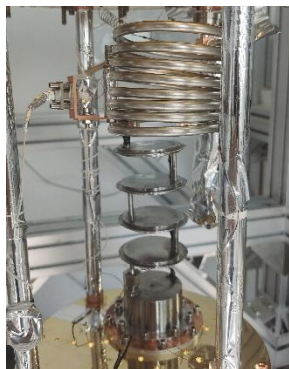


**Figure 4.** Dilution unit core components

As illustrated in Figure 4, from the top down, the unit comprises a continuous heat exchanger, a 4-stage silver powder heat exchanger, and a mixing chamber.

### 3.2. Experimental results

Throughout the entire experimental process, the total duration, including system cooling, condensation, testing, and warm-up, was consistently completed within a 60-hour period. Following the stabilization of the system's cooling state, a controlled heating procedure was implemented to elevate the circulation flow rate. Temperature measurements at the still cold plate, the concentrated phase outlet of the continuous heat exchanger, and mixing chamber cold plate were conducted using a  $\text{RuO}_2$  thermometer, with the collected data presented in Figure 5. Both the still temperature and the outlet temperature of the continuous heat exchanger were observed to increase accordingly.

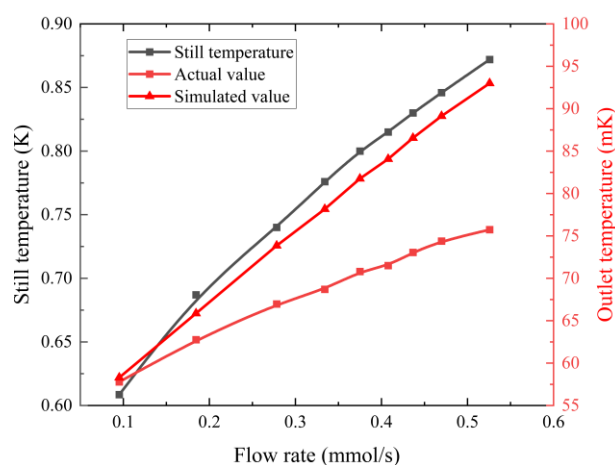


**Figure 5.** System circulating flow rate as a relation to the temperature of the still cold plate and the concentrated phase outlet of the continuous heat exchanger

In Figure 5, the gradual increase in circulating flow rate causes the still temperature and the continuous heat exchanger outlet temperature to increase synchronously. The still temperature ranges from 0.6K to 0.9K, the actual outlet temperature of the continuous heat exchanger ranges from 56mK to 78mK, and the simulated temperature is slightly higher than the actual temperature.

Analysis suggests that, in practice, the continuous heat exchanger is directly connected to the silver powder heat exchanger and mixing chamber, resulting in temperature transfer in the direction of the connection. This causes the outlet temperature of the continuous heat exchanger to be lower than the theoretical value. As the flow rate increases, the effect becomes greater, and the outlet temperature becomes lower.

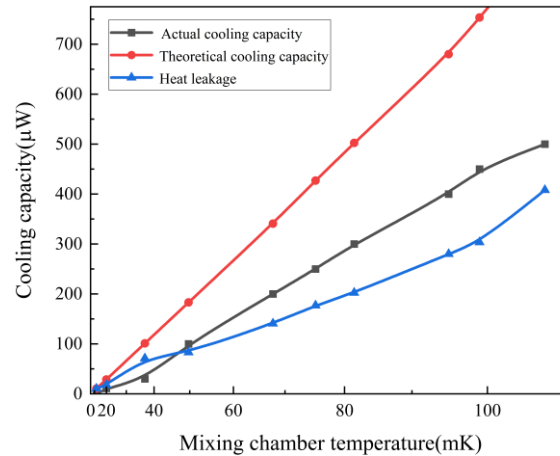


**Figure 6.** Dilution refrigerator cooling capacity

The overall system performance was subsequently evaluated. The theoretical cooling capacity was calculated using Equation (5) [7]:

$$Q = 84nT_{mc}^2 \quad (5)$$

where  $Q$  is the theoretical cooling capacity,  $n$  is the molar flow rate of  $^3\text{He}$ , and  $T_{mc}$  is the temperature of the mixing chamber. This semi-empirical model describes the cooling power of the dilution refrigerator's mixing chamber under ideal conditions.

The actual cooling capacity was obtained experimentally. The difference between the theoretical and experimental values yielded the heat leakage under various conditions, as summarized in Figure 6. The results demonstrate that the integration of the self-developed dilution unit significantly enhanced the refrigerator's performance, achieving a cooling capacity of 450  $\mu\text{W}$  at 100 mK. By modifying the support rod structure to reduce heat leakage, a cooling capacity of 500  $\mu\text{W}$  at 100 mK is anticipated.

#### 4. Conclusion

This paper analyzes the performance of a continuous heat exchanger with different flow rates and lengths through simulation calculations. It was found that the optimal length of a continuous heat exchanger should be at least 10 meters. At the same time, we developed a continuous heat exchanger with a 10-meter heat transfer length, loaded it onto a dry dilution refrigerator, and measured the outlet temperature of the continuous heat exchanger with different flow rates. It was found that the actual outlet temperature was lower than the theoretical outlet temperature. Analysis revealed that the outlet temperature of the continuous heat exchanger was affected by the thermal conductivity of the silver powder heat exchanger and the mixing chamber. Additionally, a cooling performance of 450  $\mu\text{W}$  at 100 mK was achieved with this continuous heat exchanger.

The theoretical analysis of the continuous heat exchanger presented in this paper is intended to serve as a design guide, not a detailed theoretical analysis. To carry out a specific theoretical analysis, the influence of the silver powder heat exchanger and the mixing chamber must be considered. Next, we will optimize the heat exchanger model further. On this basis, we will carry out an overall combined analysis, analyze the optimization model more systematically, and continue to optimize and improve the performance of the entire machine.

### Acknowledgments

The research is supported by the Key Research Program of the Key Laboratory of Cryogenic Science and Technology and by the Director Fund of Technical Institute of Physical and Chemical, Chinese Academy of Sciences.

### References

- [1] Zu H, Dai W, Waele A. Development of dilution refrigerators—A review. *Cryogenics*, 2021, **121**.
- [2] Wheatley JC, Vilches OE, Abel WR. Principles and methods of dilution refrigeration. *Physics*, 1968, **4**.
- [3] Oda Y, Fujii G, Ono T, et al. Practical design of heat exchangers for dilution refrigerators: part 2. *Cryogenics*, 1983, **23**.
- [4] Chaudhry G, Brisson J G. Thermodynamic Properties of Liquid  $^3\text{He}$   $^4\text{He}$  Mixtures Between 0.15 K and 1.8 K. *Journal of Low Temperature Physics*, 2009, 155(5-6)
- [5] Frossati G. Experimental techniques: Methods for cooling below 300 mK. *Journal of Low Temperature Physics*, 1992, 87(3-4).
- [6] Pradhan J, Das N K, Chakraborty A. Thermo-dynamical process simulation of dilution refrigerator. *Cryogenics*, 2013, 57
- [7] Zhao, Zuyu, and Chao Wang, eds. *Cryogenic engineering and technologies: principles and applications of cryogen-free systems*. CRC Press, 2019.